

## An independent-electron model for charge-state distributions and beam-foil populations

E. Veje

*Physics Laboratory II, H.C. Ørsted Institute, Universitetsparken 5, DK-2100 Copenhagen Ø, Denmark*

(Received 19 April 1976)

The foundations for an independent-electron model for charge-state distributions of heavy elements having passed through solids, as well as for beam-foil populations, are presented and discussed. It is proposed that the fraction  $P_i$  of particles with charge  $ie$ ,  $e$  being the charge of the proton, is given by the simple expression  $P_i = [n!/i!(n-i)!] \alpha^{n-i} (1-\alpha)^i$ , where  $n$  is the number of electrons possible outside a closed core, and  $\alpha$  is a parameter accounting for outer electrons. Modification of this expression in case the core becomes ionized is discussed. The model and its implications are compared to experimental data, and good agreement is generally found.

### I. INTRODUCTION

There has recently been some success in describing relative beam-foil population curves of helium,<sup>1</sup> beryllium,<sup>2</sup> and sulfur<sup>3</sup> in terms of two probability parameters, one accounting for Rydberg-state populations and the other describing core vacancies. Also, relations between charge-state distributions and beam-foil population curves were drawn,<sup>1</sup> the fundamental point being the empirical finding that individual levels within one level scheme to a high degree of precision have proportional population functions.<sup>1,2</sup> (With regard to the level scheme here it is understood to be the group of all energy levels of an atomic species with specified charge state and also specified core configuration.)

At present, there is no adequate theory which describes beam-foil population curves; also, experimental data are very incomplete. Therefore the finding of empirical relations governing such phenomena is of interest. The aim of this article is to define, discuss, and apply the probability factors introduced recently.<sup>1-3</sup> The results of this work need not be strictly justified physically, but until theories of more fundamental nature become available may be valuable in estimating numbers of relevance for beam-foil spectroscopy and related fields.

It is clear that beam-foil population curves, obtained by means of optical or electron spectrometry, are of more physical significance than charge-state distribution curves, when autoionizing levels<sup>4</sup> are populated to non-negligibly small amounts. This is not only because beam-foil spectrometry yields specific information on population of a selected level, or in some cases even a magnetic substate, but also because population of autoionizing levels can introduce an ambiguity in charge-state distribution observations. Their presence will change the beam composition to

higher charge states with increasing distance downstream from the foil. This has been observed directly by Dmitriev *et al.*,<sup>5</sup> who measured changes in charge fractions of lithiumlike ions of the elements Be, B, C, N, and O, and, generally, relatively strong populations of multiply excited species are observed in beam-foil studies.<sup>2,6,7</sup>

Until now, only a few experimental and theoretical attempts to investigate the beam-foil excitation mechanism have been made. Much more effort has been put into the understanding of charge-state distributions. In 1972 Betz reviewed very thoroughly the experimental and theoretical situation concerning charge states of heavy ions having penetrated solids as well as gasses.<sup>8</sup> In that monograph surveys of theoretical considerations prior to 1972 are given, and they shall therefore not be repeated here.

In Sec. II we shall mention a few experimental facts which serve as foundations for the independent-electron model. The model is presented in Sec. III, and it will be applied to experimental data in Sec. IV. The results will be discussed and compared to other models in Sec. V.

### II. FOUNDATIONS FOR THE INDEPENDENT-ELECTRON MODEL

Brandt has recently discussed ion screening in solids.<sup>9</sup> He concludes that protons cannot bind an electron inside a normal metal at any velocity. Heavier projectiles carry an electron cloud which at low velocities screens dynamically the ion charge, but which at higher velocities cannot follow the motion of the projectile, and the electrons are stripped off. Brandt specifies that the mean charge of a projectile inside the solid appears as a parameter which, in general, depends on the phenomenon studied. Charge states of ions after emergence from a solid are determined by the correlation gain of electrons inside the solid in

scattering collisions with the moving ion, by the inner-shell excitation of the moving ion core, and by the effects of the electronic "salvage" at the target exit surface.

Garcia has shown<sup>10</sup> that any highly excited state in a weakly ionized atom cannot exist during the passage through the solid. This fact is directly related to the geometrical size of the electronic orbitals, and it will also hold for valence-shell states and low-lying excited states to a good approximation.

Fortner and Garcia<sup>11</sup> have recently determined from x-ray measurements the *M*-shell vacancy distribution for argon ions *inside* a graphite target in the projectile energy range 30–200 keV. They compared their results with those from a charge-state distribution measurement performed after the projectiles had left the solid, and they concluded that differences in the two distributions indicate a dramatic rearrangement of the ion near the back surface of the foil. They found that the charge-state distribution after passage out of the solid is skewed to *fewer* vacancies than those present inside the solid, and they concluded that a large probability of electron capture at the exit surface could account for these differences.

Recently, in optical beam-foil observations, the angle between the beam axis and the foil normal has been varied by rotating the foil, and changes in polarization of optical line radiation have been observed.<sup>12</sup> Variation of a measured quantity with tilt angle indicates the presence of surface effects in the beam-foil excitation mechanism, because the interior of an amorphous foil is not changed by tilting the foil. The tilt angle is defined only through the presence of a surface.

Datz *et al.*<sup>13</sup> have observed electron-exchange phenomena at the front surface as well as at the back of the foil in channeling experiments. This also indicates the role of the surface in beam-foil experiments.

Consequently, the final arrangement of electrons outside a core of fairly small size compared with the average distance between nearest nuclei in the solid must take place during the time that the particle interacts with the back of the foil. This interaction can be regarded as electron transfer or electron capture from the back of the foil to the projectile.

When the projectile leaves the foil, it will be followed by a cloud of electrons.<sup>14</sup> This results in a local, net positive charge on the foil at or around the projectile exit. The electrons following the projectile will therefore feel a rather strong attractive force back to the foil, at the same time as they are influenced by the attraction

from the core of the projectile. Both of these attractive forces will most often be caused by several positive-charge units; thus the mutual electron-electron repulsion will be much smaller. To the extent that this electron-electron repulsion can be ignored, compared with the two above-mentioned attractive forces, the electrons will be transferred (or not transferred) from the foil to the projectile as independent particles, and the problems of the beam-foil excitation mechanism are accordingly reduced to those of a one-electron system.

If the mutual electronic repulsion becomes comparable to the two attractions, the independent-electron picture will not necessarily be a good approximation. It will, however, still be valid to some extent as long as the coupling among the electrons is not very great, and that will rarely happen.

From the above we shall propose a model which regards an atom as made up of two parts: (i) a core of inner shells of relatively small size, which can lose electrons only during rather violent collisions with an atom in the solid, but which can pick up electrons also at the exit, and (ii) the valence shell together with outer shells, which are all ill-defined during the passage through the solid. We shall apply an independent-electron picture to the arrangement of electrons outside the core.

Similar ideas to the one outlined above have been introduced in the theory of electron capture of  $\alpha$  particles by Oppenheimer,<sup>15</sup> as well as in other fields of physics like photoionization,<sup>16</sup> shakeoff,<sup>17</sup> and atomic collision phenomena.<sup>18</sup> The ideas behind this reduction to an independent-electron picture can indeed be traced back beyond Schrödinger's description by means of wave functions to the early picture by Bohr and Sommerfeld, and these ideas result in the independent-particle model.<sup>19</sup> Thus it is reasonable, as a starting point in the treatment of the beam-foil excitation mechanism, to assume that the electrons are transferred (or not transferred) independently.

The beam-foil model outlined above has the following immediate implications: Since the population of Rydberg states happens as the projectile leaves the foil, it is reasonable to expect that Rydberg-state population will be influenced by the form of the electronic wave functions in the vicinity of the projectile nucleus, from the time of emergence until the atom is completely free. It is well known<sup>20</sup> that for different members of the same atomic Rydberg series the inner parts of their wave functions are proportional, the proportionality factor being  $n^{-3/2}$ , where  $n$  is the principal quantum number. This explains why

the term population within the same term series goes asymptotically as  $n^{-3}$ , as found experimentally,<sup>1</sup> because the population probability is proportional to the square of the amplitude of the wave function. At the same time it also explains why different members of the same series have proportional beam-foil population functions,<sup>1,2</sup> and it justifies the empirical factorization<sup>2</sup> of beam-foil level populations into a product of a factor accounting only for kinematics and a factor accounting only for all quantum numbers of the resultant specific excited level in question [cf. Eq. (2) of Ref. 2]. Furthermore, since the amplitude of a helium triplet wave function in the vicinity of the nucleus is smaller than the amplitude of the corresponding singlet wave function,<sup>21</sup> the above argument also explains why the ratio of the population of a triplet to that of the corresponding singlet is smaller than 3, as observed for heliumlike species.<sup>2,22</sup>

Thus various beam-foil observations are explained from basic properties of the final Rydberg-state wave functions. This is in line with the explanation of similar trends found in ion-atom collisions.<sup>23</sup>

### III. DEFINITIONS AND EQUATIONS OF THE MODEL

In the following a monochromatic beam of swift atomic particles having just passed through a thin solid foil is considered.

Let  $P_i$  denote the fraction of particles which carry the charge  $ie$ ,  $e$  being the charge of a proton.  $P_i$  can be regarded as the probability that a particle ends up with the net total charge  $ie$ . Obviously

$$\sum_j P_j = 1, \quad (1)$$

where the summation is carried out over all possible charge states  $j$  of the projectile.

Now first regard a projectile with a completely filled core which remains undisturbed during the passage through the solid, and with the possibility of accommodating up to but not more than  $n$  electrons outside the closed core. The case of possible core vacancies will be treated later. We shall define a parameter  $\alpha$  as the total probability that an electron is transferred from the back of the foil to a bound state outside the core. The state can be either a Rydberg state or a valence-shell level, since all of these states are found to have the same kinematical dependence, as discussed in Sec. II and in Refs. 1 and 2. The probability that an electron is not transferred is of course  $1 - \alpha$ .

Following the independent-electron picture out-

lined in Sec. II, it is then easy to show, by use of basic laws of probability, that the charge-state fraction  $P_i$  is given by

$$P_i = [n! / i!(n-i)!] \alpha^{(n-i)} (1-\alpha)^i. \quad (2)$$

This is a binomial probability distribution, discussed in most statistics or probability texts. It reflects the extreme of an independent-electron picture, and a possible justification of the model will stem from agreements between experimental data and Eq. (2).

Equation (2) links  $n+1$  charge-state components by use of only one parameter,  $\alpha$ , which at present has to be determined from experiment. Clearly, any set of charge fractions given by Eq. (2) will fulfill Eq. (1).

The parameter  $\alpha$  may be introduced in a somewhat different way. It need not be assumed that the arrangement of outer electrons happens at the same time at the back of the foil. However, if it is assumed that the arrangement happens during the passage through the solid as an equilibrium result of various processes, then to reach Eq. (2) one must assume that the different electron-capture and -loss processes have the same probabilities, regardless of the charge state of the projectile. This assumption is, however, unjustified. Rather, one should assume that each electron has its own value of  $\alpha$ . Such an idea has been outlined by Dmitriev,<sup>24</sup> and the fundamental difference between that work and the model proposed here is that here all outer electrons are treated as equivalent particles.

From Eq. (2) one obtains

$$\frac{dP_i}{dv} = \frac{n(1-\alpha) - i}{\alpha(1-\alpha)} P_i \frac{d\alpha}{dv}, \quad (3)$$

where  $v$  is the projectile velocity. There are reasons to believe that  $\alpha$  is a monotonically decreasing function of  $v$  for all velocities, (see Refs. 1-3 and the results of Sec. IV). This implies that the maximum value for  $P_i$  [which will be denoted  $(P_i)_{\max}$ ] occurs at

$$\alpha = 1 - i/n, \quad (4)$$

which by use of Eq. (2) yields

$$(P_i)_{\max} = \frac{n!}{i!(n-i)!} \left(1 - \frac{i}{n}\right)^{n-i} \left(\frac{i}{n}\right)^i. \quad (5)$$

Note that nothing has been said about the velocity at which  $(P_i)_{\max}$  occurs.

Furthermore, as a curiosity,

$$\lim_{n \rightarrow \infty} (P_i)_{\max} = e^{-i} i^i / (i!).$$

For  $P_i = (P_i)_{\max}$ , Eq. (2) yields

$$(P_i)_{\max} = [(i+1)/i] P_{i+1}. \quad (6)$$

The mean charge  $\langle i \rangle$ , defined

$$\langle i \rangle \equiv \sum_i i P_i, \quad (7)$$

is found to be

$$\langle i \rangle = n(1 - \alpha), \quad (8)$$

a relation which is obvious, once it has been derived. The width  $\sigma$ , defined

$$\sigma \equiv \left( \sum_i (i - \langle i \rangle)^2 P_i \right)^{1/2},$$

is given by

$$\begin{aligned} \sigma &= [n(1 - \alpha)\alpha]^{1/2} \\ &= (\langle i \rangle \alpha)^{1/2}. \end{aligned} \quad (9)$$

The situation becomes more involved in cases where core excitation, too, can take place. Whereas the outer electrons can be treated by use of only one probability factor, namely,  $\alpha$ , each subshell of the core will presumably have its own distinct vacancy probability factor.<sup>25</sup> If only one inner shell undergoes ionization, one can introduce a factor  $\beta$  as the total probability that a vacancy exists in the core of the projectile as it leaves the foil. Then it is easy to express in terms of  $\alpha$  and  $\beta$  the probability  $P_{i,\iota}$  that the projectile, after having traversed the solid, has  $\iota$  core vacancies out of  $\nu$  possible ones and that  $i$  outer electrons out of  $n + \iota$  are missing. One arrives at the expression

$$\begin{aligned} P_{i,\iota} &= \frac{\nu!}{\iota!(\nu - \iota)!} \beta^\iota (1 - \beta)^{\nu - \iota} \\ &\times \frac{(n + \iota)! \alpha^{(n + \iota - i)} (1 - \alpha)^i}{i!(n + \iota - i)!}, \end{aligned} \quad (10)$$

which is a product of two binomial distributions.

Here I have used the fact that multiple-vacancy production tends to be the result of a single step-excitation process,<sup>18,25,26</sup> and it is assumed that electron capture from the back of the foil to the projectile core can be treated in the independent-electron picture. Such processes are included in  $\beta$  by definition, which implies that values of  $\beta$  deduced from beam-foil experiments are not directly comparable to core-vacancy determinations from x-ray measurements on projectiles inside solids.

The total fraction of ions with a certain charge is obtained by summing all possible probability terms leading to the same net charge. However, as mentioned above, the concept of charge fractions loses the clear physical meaning it has in cases for which no core excitation occur, because of autoionizing processes.

Obviously

$$\sum_{i,\iota} P_{i,\iota} = 1. \quad (11)$$

In analogy with Eq. (8) one obtains for the mean charge  $\langle i + \iota \rangle$  the relation

$$\langle i + \iota \rangle = n(1 - \alpha) + \nu\beta. \quad (12)$$

For some combinations of  $i$  and  $\iota$ ,  $P_{i,\iota}$  will be a probability for ending up with excited levels of an entire level scheme, whereas in other cases  $P_{i,\iota}$  will be the probability of getting only a single state or getting a bare nucleus. As an example, in helium all singly excited, neutral He levels are treated together, whereas the ground state of neutral helium is treated separately.<sup>1</sup> We suggest that the totality of levels of an element which are treated together in one specific combination of  $i$  and  $\iota$  [cf. Eq. (10)] shall be called one *variety* of that element. A variety can thus be an entire set of excited levels, or even all displaced terms together with normal terms (cf. Be I<sup>a</sup> and Be I<sup>b</sup> in Ref. 2), it can be one single state, or even a bare nucleus. Thus there are six varieties of helium,<sup>1</sup> whereas there are only three charge components and only three level schemes.

The term variety is here introduced in analogy with its use for classification in other natural sciences, and its use here will be further demonstrated in Sec. IV under the treatment of lithium (Table I).

For up to  $n$  outer electrons and up to only two electrons in the core (i.e., the completed core is of configuration  $s^2$ ) there are  $3n$  varieties but only  $n + 3$  different charge states. Both the total set of charge states, as well as that of varieties, are linked with one obvious relation, Eqs. (1) or (11), respectively.

#### IV. APPLICATION OF THE MODEL TO EXPERIMENTAL DATA

##### A. General remarks

In this section the model outlined above shall be compared to experimental data. Only the elements He, Li, Be, and S have been studied in detail by use of beam-foil spectrometry.<sup>1-3</sup> Experimental charge-state distributions at low and medium energies are available for all of the lighter elements except Be. Of the data published, those given by Hvelplund *et al.*<sup>27</sup> are particularly applicable to the model proposed here, because Hvelplund *et al.* carefully selected only particles which were scattered less than  $0.3^\circ$  during the passage through the foil, and in that way depressed contributions from particles with core vacancies. Also, they determined the energy losses, so that their charge-state distribution data are

given as a function of emergent beam-energy. All of the experiments referred to in the following have been performed on ions traversing thin self-supporting carbon foils. All values of  $\alpha$  and  $\beta$  referred to here and in Refs. 1–3 have been obtained by the method of trial and error, and as the curve fitting has not been optimized formally in any case, a parameter choice slightly different from the ones chosen might cause slightly better agreement between the experimental data and the model.

### B. Hydrogen

For hydrogen three varieties exist, but they reduce to two charge-state distributions which are related through Eq. (1). Thus only one parameter can be deduced from experimental data, making an analysis in terms of two parameters senseless. However, since Brandt has concluded<sup>9</sup> that protons cannot bind an electron inside a solid at any velocity (this corresponds to  $\beta=1$ ), and since even the ground state of hydrogen is a Rydberg state, the total creation of neutral hydrogen can be regarded as resulting from electron transfer at the back of the foil. Consequently, one arrives at the two following relations for the two charge components for hydrogen:

$$P_0 = \alpha, \quad P_1 = 1 - \alpha.$$

Charge-state distribution data observed in transmission have been reported by Chateau-Thierry and Gladieux.<sup>28</sup> Buck *et al.* give data from back-scattering experiments,<sup>29</sup> which essentially agree with the transmission data. From these data sets  $\alpha$  can immediately be found. Though this is trivial, the result may contribute to systematic trends of  $\alpha$ , and therefore the average results are shown in Fig. 1. Also, Brandt and Sizmann<sup>30</sup> have explained theoretically the charge-state distributions of hydrogen at velocities comparable to the Fermi velocity as electron capture from the tail of the electron distribution at the target surface. This is essentially in accordance with the independent-electron model, and it may indicate how to estimate  $\alpha$  theoretically.

### C. Helium

Beam-foil population curves and charge-state distributions for He below 300 keV have recently been analyzed<sup>1</sup> in terms of the two parameters  $\alpha$  and  $\beta$ , which were found to reproduce satisfyingly well three sets of beam-foil population curves, the three charge-state components, and one beam-foil absolute population measurement in neutral helium performed at 275 keV. In Ref. 1 also the ambiguity caused by autoionizing levels

was discussed.

In Ref. 1 the value of  $\beta$  was found to be larger than 0.9 for projectile energies above 500 keV. Since the fraction of bare helium nuclei is given by the product  $\beta^2(1-\alpha)^2$  it is possible to estimate the value of  $\alpha$  for energies well above 500 keV by setting  $\beta=1$  and by use of the experimental charge-state fraction data of Armstrong *et al.*<sup>31</sup> The results are shown in Fig. 1, which also contains the data of Ref. 1. The two data sets for He given in Fig. 1 have been obtained quite differently. The low-energy data come from optical measurements performed immediately after the foil on electron-carrying species, whereas the charge-state analysis of Armstrong *et al.* was performed 1 m downstream only on particles which had suffered almost no deflection during passage through the foil. Therefore Fig. 1 does not necessarily give more than gross structure behavior for  $\alpha$  for helium, although the two sets of measurements yield values which join each other smoothly.

It is worth noting that the hydrogen and the helium data are rather similar. In the high-velocity limit they both decrease in a manner close to a  $v^{-4}$  dependence, where  $v$  is the projectile velocity. Also, it is seen that in the velocity region 1–2 a.u., the rate of decrease of  $\alpha$  for helium lessens. This may be a velocity-matching phenomenon.

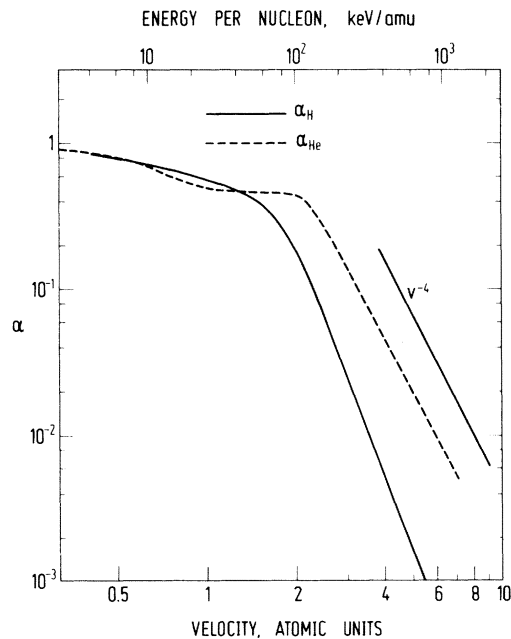


FIG. 1. Values of  $\alpha$  for hydrogen and helium obtained as described in the text, plotted in a log-log plot vs the projectile velocity in a.u. (bottom abscissa scale) or vs the projectile energy per nucleon (top abscissa scale). Also, a  $v^{-4}$  dependence is shown by the straight line.

TABLE I. Probability formulas as used in the text for the analysis of the lithium beam-foil data given by Andersen *et al.* (Ref. 32). Note that  $n, n',$  and  $n''$  denote here principal quantum numbers  $\geq 2$ ;  $l, l',$  and  $l''$  are azimuthal quantum numbers.

Variety	Configuration	Probability in terms of $\alpha$ and $\beta$
Li I <sup>a</sup>	$1s^2nl$	$\alpha(1-\beta)^2$
Li I <sup>b</sup>	$1sln'l'$	$2\alpha^2\beta(1-\beta)$
Li I <sup>c</sup>	$nl'n'l''l''$	$\alpha^3\beta^2$
Li II <sup>g</sup>	$1s^2$	$(1-\alpha)(1-\beta)^2$
Li II <sup>a</sup>	$1snl$	$4\alpha(1-\alpha)\beta(1-\beta)$
Li II <sup>b</sup>	$nl'n'l'$	$3\alpha^2(1-\alpha)\beta^2$
Li III <sup>g</sup>	$1s$	$2(1-\alpha)^2\beta(1-\beta)$
Li III <sup>e</sup>	$nl$	$3\alpha(1-\alpha)^2\beta^2$
Li <sup>3+</sup>		$(1-\alpha)^3\beta^2$

#### D. Lithium

Andersen *et al.*<sup>32</sup> have measured relative beam-foil population curves for Li I<sup>a</sup>, Li I<sup>b</sup>, and Li II<sup>a</sup> levels in the energy range 10–75 keV. In Table I are given probability factors for the different varieties of lithium, expressed in terms of  $\alpha$

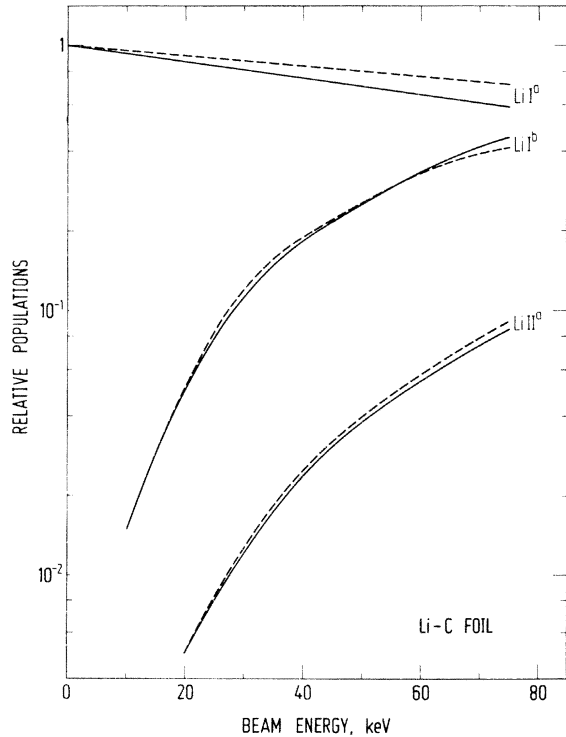


FIG. 2. Relative beam-foil population curves for Li I<sup>a</sup>, Li I<sup>b</sup>, and Li II<sup>a</sup> terms. The solid curves are experimental data taken from Andersen *et al.* (Ref. 32), and the dashed curves result from the values of  $\alpha$  and  $\beta$  shown in Fig. 3.

and  $\beta$ . It is easy to reproduce the three sets of population curves of Andersen *et al.* by use of the relevant expressions of Table I. This is demonstrated in Fig. 2, in which the population curves reported by Andersen *et al.* are given by solid curves, and the dashed curves are results obtained by use of the values of  $\alpha$  and  $\beta$  shown in Fig. 3.

#### E. Beryllium

Beryllium has been studied by the beam-foil technique in the energy range 60–360 keV. Five sets of population curves have been reproduced satisfyingly well by use of only the two parameters  $\alpha$  and  $\beta$ , as discussed by Dynefors *et al.*<sup>2</sup> Indeed, those findings, together with the data for helium<sup>1</sup> and sulfur,<sup>3</sup> initiated this work.

#### F. Boron

Bickel *et al.*<sup>33</sup> measured charge-state distributions of boron ions passing through carbon foils in the energy range 0.25–1.75 MeV. They found at 1.75 MeV the fraction of B<sup>4+</sup> was only 5%, indicating that K-shell vacancies can be ignored in analyzing their data. Therefore Eq. (2) can be applied with the possibility of only up to three

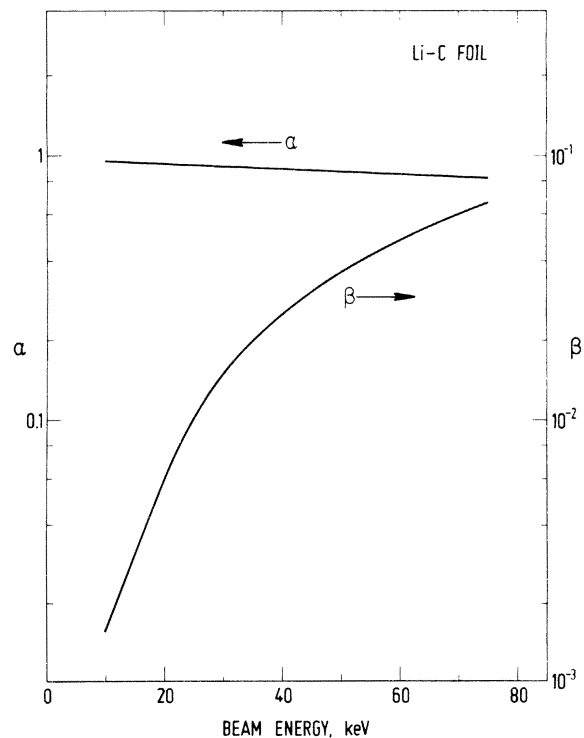


FIG. 3. Values of  $\alpha$  and  $\beta$  used in the evaluation of the dashed curves shown in Fig. 2, as function of the projectile energy in front of the foil.

electrons outside the completed  $1s^2$  core.

At any energy below 1.75 MeV, the data sets of the four charge fractions of boron<sup>33</sup> can be reproduced well by the values of  $\alpha$  shown in Fig. 4 and the relevant versions of Eq. (2), except that the experimentally determined fraction of neutrals at low energies is systematically lower than that predicted from the relative distributions of +1, +2, and +3 charged particles and Eq. (2). If it is assumed that the neutral component shall approach unity for projectile velocities approaching zero, then an extrapolation of the fraction of neutrals given by Bickel *et al.*<sup>33</sup> shows an abrupt increase with decreasing projectile energy, indicating that the neutral component reported by them may be systematically too low.

#### G. Carbon

Charge-state distribution measurements have been performed by Smith and Whaling<sup>34</sup> at energies from 369 to 1450 keV, and by Girardeau *et al.*<sup>35</sup> from 1 to 5 MeV. At these rather high energies, the  $1s^2 2s^2$  core can undergo ionization, so that core excitations have to be taken into account. Therefore beam-foil population curves rather than charge-state distributions are required to test the model. Unfortunately, the sparse beam-foil population measurements of Poulizac *et al.*<sup>36</sup> (0.4–2.0 MeV) do not permit a detailed analysis. It can be said at present only that the reported charge-state distribution data,<sup>34</sup> together with

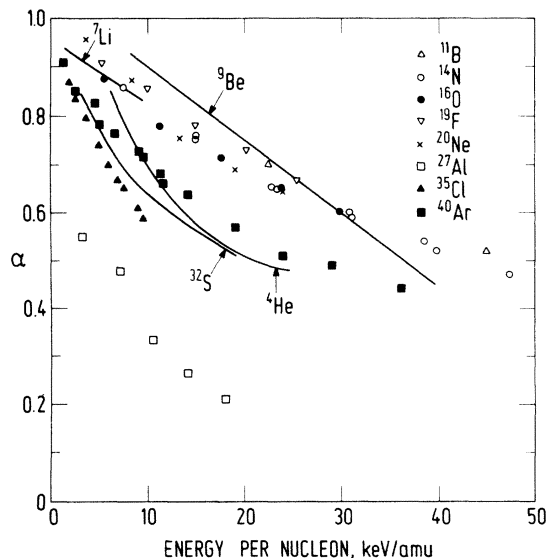


FIG. 4. Values of  $\alpha$  for the elements He, Li, Be, B, N, O, F, Ne, Al, S, Cl, and Ar, obtained as described in the text. Abscissa gives the projectile energy per nucleon. The curves for He, Be, and S have been taken from Refs. 1–3, respectively.

the beam-foil data,<sup>36</sup> are not in conflict with the model proposed. A detailed beam-foil study of this element seems at present to be justified, since it can yield considerable information.

#### H. Nitrogen

Hvelplund *et al.*<sup>27</sup> performed charge-state distribution measurements in the energy interval 89–479 keV, Smith and Whaling<sup>34</sup> report data from 180 to 1450 keV, and Girardeau *et al.*<sup>35</sup> give information from 1 to 5 MeV. The different data sets agree very well where they overlap. The charge-state distribution curves are followed by one N II and one N III beam-foil population measurement<sup>37</sup> in the energy range where the  $1s^2 2s^2$  core remains unexcited. This is in agreement with the model proposed.

The  $1s^2 2s^2$  core is practically undisturbed at projectile energies below 600 keV, reducing the charge-state distributions to essentially those of a three-electron system. Indeed, the experimental charge-state distributions are in this energy region described very well by the four appropriate versions of Eq. (2) and the values of  $\alpha$  shown in Fig. 4. This is demonstrated in Fig. 5, in which the experimental values (shown by crosses<sup>27</sup> or open circles<sup>34</sup>) are compared to the results (shown by full circles) obtained from Eq. (2) and the values of  $\alpha$  given in Fig. 4. The solid curves of Fig. 5 are only guides to the eye. Even up to energies as high as 1.2 MeV, the four charge-state fractions are linked well by only one parameter, in spite of the fact that  $P_4$ , which involves  $1s^2 2s^2$  core ionization, reaches values as high as 5–10% (cf. Fig. 5).

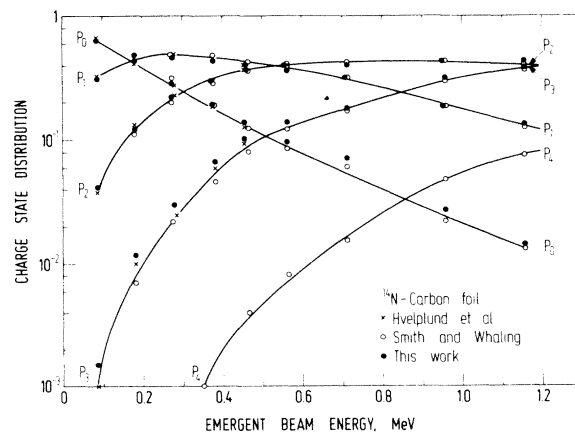


FIG. 5. Charge-state components for nitrogen. Experimental values are shown by crosses (Ref. 27) or open circles (Ref. 34). The values obtained by use of Eq. (2) and the values of  $\alpha$  given in Fig. 4 are given by full circles. The curves are guides to the eye only.

### I. Oxygen, fluorine, and neon

For these three elements also, charge-state distributions have been determined by Hvelplund *et al.*<sup>27</sup> at energies where core excitations are very small. The experimental data are reproduced well by treating them as systems of four, five, and six electrons, respectively, and by use of the values of  $\alpha$  given in Fig. 4. This is demonstrated for neon in Fig. 6.

Girardeau *et al.*<sup>35</sup> report experimental charge-state distribution data for oxygen and neon above 1 MeV. Unfortunately,  $P_0$  is missing in this data set, but since this component is very small at these energies, its omission does not influence the interpretation appreciably. Even at energies up to approximately 2 MeV the charge-state distributions of oxygen and neon are well described by use of Eq. (2). The values for  $\alpha$  at high energy are smooth continuations of those found at lower energies (cf. Fig. 4). Also, neon beam-foil population curves<sup>37</sup> follow closely the relevant charge-state distribution curves up to  $\sim 2$  MeV. Thus in conclusion oxygen, fluorine, and neon confirm the model as well as nitrogen does.

### J. Sodium and magnesium

The charge-state distributions of Hvelplund *et al.*<sup>27</sup> indicate that for these elements core excitations have to be taken into account even at energies around 100 keV. This is in agreement with observation<sup>38</sup> of a transition between doubly excited Na I levels even down to a projectile energy of 30 keV, and a transition between doubly excited Mg II levels seen<sup>6</sup> at 150 keV.

For these two elements, the situation is similar to that of carbon, and here also, beam-foil data

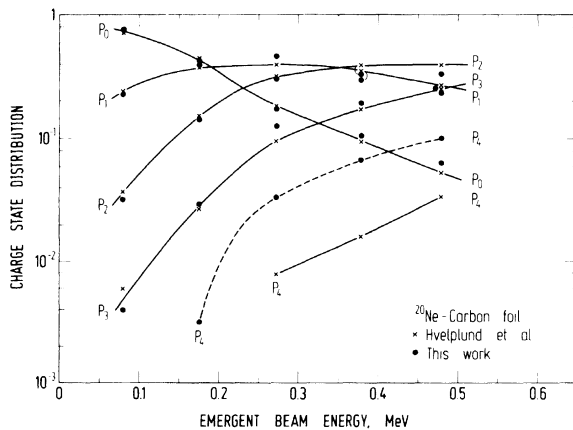


FIG. 6. Charge-state distributions for neon. Experimental values (Ref. 27) are shown by crosses, and the results obtained from the model are shown by full circles. The curves are guides to the eye only.

can yield valuable information. As a curiosity, it can be mentioned that the magnesium data<sup>27</sup> can be fitted well by a three-electron system.

### K. Aluminium

For this element, a three-electron system reproduces the data of Hvelplund *et al.*<sup>27</sup> very well, similarly to nitrogen. The values of  $\alpha$  are included in Fig. 4.

### L. Sulfur

Beam-foil measurements on sulfur have been reported and analyzed elsewhere.<sup>3</sup> Therefore the results, which are in agreement with the model, shall not be repeated here. The values obtained for  $\alpha$  are included in Fig. 4.

Berry *et al.*<sup>39</sup> report a charge-state distribution measurement at 1 MeV. Their data are fitted well by  $\alpha = 0.34$  (see Fig. 7).

### M. Chlorine and argon

Charge-state distributions for chlorine and argon have been measured by Turkenburg *et al.*<sup>40</sup> in the energy range 70–350 keV. The argon data agree well with those of Hvelplund *et al.*,<sup>27</sup> who measured up to 450 keV, and with those of Smith and Whaling,<sup>34</sup> who measured up to 1450 keV.

The data reported for these two elements agree well with the model proposed, treated, respectively, as systems of five and six electrons. This is demonstrated for argon in Fig. 8. The values for  $\alpha$  are included in Fig. 4.

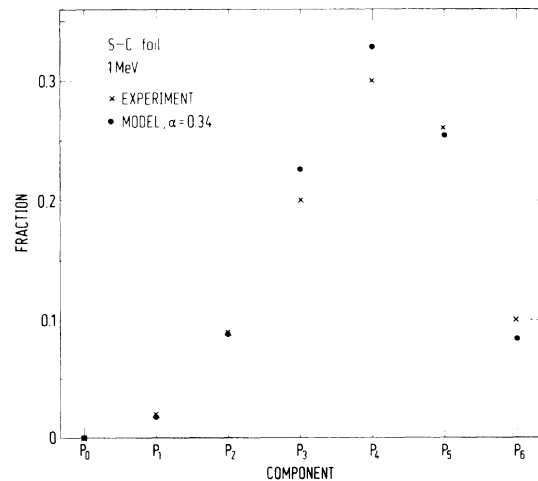


FIG. 7. Charge-state components for sulfur at 1 MeV. Experimental values (Ref. 39) are shown by crosses and the values obtained by use of Eq. (2) with  $\alpha = 0.34$  are given by full circles.



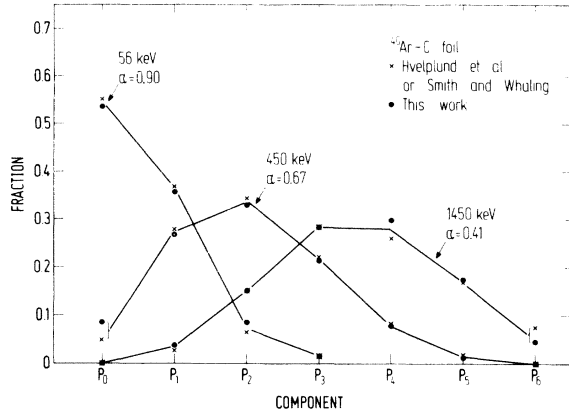


FIG. 8. Charge-state fractions for argon at 56, 450, and 1450 keV. The experimental values (Refs. 27, 34) are shown by crosses, and the results of Eq. (2) and the values of  $\alpha$  given in the figure are indicated by full circles.

### V. DISCUSSION

The values of  $\alpha$  obtained by the analysis performed in Sec. IV are given in Fig. 4., in which the abscissa used is the projectile energy per nucleon. Included are also the results of the previous helium,<sup>1</sup> beryllium,<sup>2</sup> and sulfur<sup>3</sup> studies, shown by solid curves.

First, it is striking to see the closeness for  $\alpha$  for the elements nitrogen through neon. This is also demonstrated in Fig. 9, in which the neutral fractions  $P_0$  for nitrogen and neon are calculated by use of the *average* value of  $\alpha$  for the first-row elements (Fig. 4.) and the relevant versions of Eq. (2), which are  $P_0 = \alpha^3$  and  $\alpha^6$ , respectively. The results of this calculation are given by solid curves in Fig. 9, and the experimental results of Hvelplund *et al.*<sup>27</sup> are given by circles for nitrogen and by crosses for neon. As can be seen, the overall agreement is good.

This empirical fact that the elements nitrogen through neon have essentially the same variation of  $\alpha$  with projectile velocity may indicate that for these elements the variation of  $\alpha$  with projectile velocity is given by the nature and number of the states available rather than by the effective or net charge of the core. This need not be a surprise, since for these elements with the same core an electron which is transferred to a state outside the core will have the same precursors and the relative shape of these will be the same, no matter what the charge of the nucleus is.

While the scaling of  $\alpha$  with projectile element thus seems to be straightforward for the first-row elements, the scaling of  $\alpha$  for heavier elements may be somewhat different, because of the relative displacements of atomic levels with

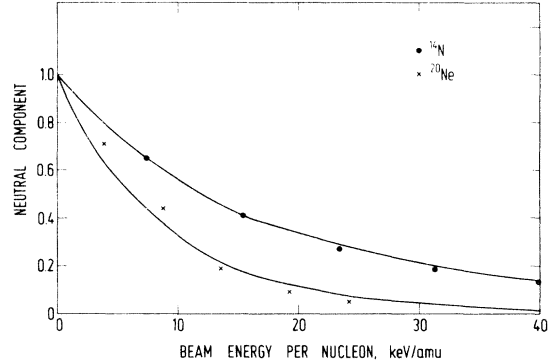


FIG. 9. Neutral components for nitrogen and neon as a function of the projectile energy per nucleon. Experimental values (Ref. 27) are shown by crosses or circles, and the curves are obtained from Eq. (2) by using the average values of  $\alpha$  given in Fig. 4 for the first-row elements.

atomic number. However, for heavy elements, the Thomas-Fermi statistical model will apply as the limiting case. Bohr has argued<sup>41</sup> that in that limit, and for projectile velocities  $v$  in the interval  $v_0 < v < Z_1^{2/3} v_0$  ( $v_0$  being the classical velocity of the electron in the ground-state hydrogen atom, and  $Z_1$  the projectile atomic number), the mean charge is given by the simple formula  $vZ_1^{1/3}/v_0$ . This is reflected in experimental values for mean charges.<sup>8</sup> This property, together with Eq. (8), can be of use in estimating  $\alpha$  values. To test this, we have in Fig. 10 plotted the mean charge calculated as  $n(1 - \alpha)$  [cf. Eq. (8)] for N, O, Ne, Al, S, and Ar versus  $Z_1^{1/3}(E/M)^{1/2}$ ,  $M$

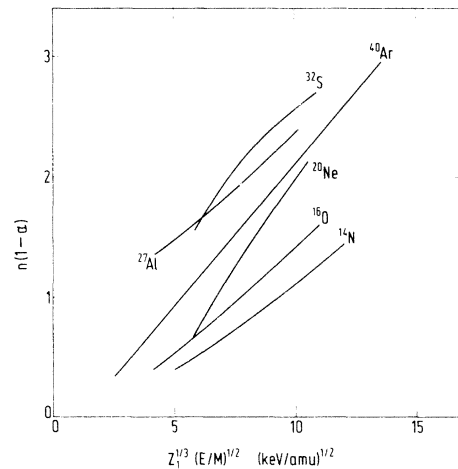


FIG. 10. Mean charge calculated as  $n(1 - \alpha)$  as a function of  $Z_1^{1/3}(E/M)^{1/2}$ , where  $Z_1$  is the projectile atomic number, and  $E$  and  $M$  are the projectile energy in keV and the mass in atomic units, respectively. The values for  $\alpha$  have been obtained by drawing smooth curves through the relevant data points given in Fig. 4.

being the projectile mass. It is seen that the data for the elements Ne, Al, S, and Ar seem to merge to one common curve for velocities so large that the relation  $v_0 < v$  is fulfilled. It is worth noting in Fig. 10 that the data for aluminium come close to those for neon as well as to those for argon. This is not the case when  $\alpha$  is plotted versus the projectile velocity, as in Fig. 4, where the Al-data are remarkably low. Unfortunately, at the time of writing, no beam-foil data are available for elements heavier than argon and for velocities larger than  $v_0$ . Figure 10 clearly expresses the need for such data.

The light elements N and O have their individual curves in Fig. 10. This is to be compared to the above-mentioned and explained fact that the  $\alpha$  values for the first-row elements come close to becoming one curve in Fig. 4.

Scaling properties for inner-shell excitations in atomic-collision phenomena are discussed in Ref. 42. However, at the moment  $\beta$  has been determined for the very light elements He, Li, and Be only. Therefore it is not yet known whether scaling laws similar to those discussed in Ref. 42 are applicable to resultant inner-shell excitations in beam-foil interactions. Especially, there may be a substantial electron pickup from the back of the foil and into the inner shells of the projectile. There seems at present to be some experimental evidence for such an electron pickup:

(i) Datz *et al.*<sup>13</sup> observed electron pickup at the front surface as well as at the back in channeling experiments.

(ii) Baragiola *et al.*<sup>43</sup> have recently measured absolute yields of argon *L* Auger electrons produced by Ar projectiles emerging from carbon foils in the projectile energy range 100–800 keV. They found the fraction of beam particles with a *2p* vacancy substantially smaller than that determined by Fortner and Garcia<sup>11</sup> from x-ray yields emitted inside the solid. This may indicate a large probability for electron pickup from the back of the foil and into the *2p* projectile shell.

(iii) In the beam-foil study using sulfur<sup>3</sup> we were unable to observe any optical transitions of ionic species with a hole in the *2p* shell even at 600 keV, in spite of the high sensitivity of the optical equipment, and although Fortner and Garcia<sup>11</sup> observed x rays from the filling of argon *2p* vacancies. This also may indicate a substantial probability for electron pickup into the *2p* shell inside or at the back of the foil. Such electron transfer processes must also be included in a theoretical estimate of a possible scaling law for  $\beta$ , and clearly further experimental data are called for, together with theoretical work.

The maximum values of each charge-state component are given by Eq. (5), and in Table II are given the maximum values predicted by the model compared with those found experimentally. As can be seen, the agreement between experimental and theoretical values is generally quite good. The disparities of boron have been mentioned previously, with the suggested explanation that the experimental values for the neutral fraction are systematically low.

It is worth noting that the model predicts the maximum value of a charge-state component without any information about at which projectile velocity the extremum occurs.

The comparison between experimentally found maximum values and those predicted by the model does not yield any confirmation of the model independent of that discussed in Sec. IV. Agreements between sets of values shown in Table II reflects only the reasonably good fitting of points given in Figs. 5–8.

Equation (2) is clearly able to reproduce an asymmetric charge-state distribution such as that of argon at 56 keV (cf. Fig. 8). This is superior to the Gaussian distribution,<sup>8</sup> which was introduced as an approximate description when the mean charge-state is large. Also, shell effects, which result in skewed distributions,<sup>8</sup> can be accounted for by inclusion of core-vacancy probability factors.

Garcia<sup>10</sup> has recently discussed the particle-foil interaction from a statistical approach based on an equilibrium description similar to that for

TABLE II. Comparisons between the experimentally and theoretically determined maximum values for the different charge-state components. The experimental data are average values of the numbers given in the different references mentioned in the text.

Element	Source	Charge-state component				
		$P_1$	$P_2$	$P_3$	$P_4$	$P_5$
B	Expt.	0.59	0.53			
	Theor.	0.44	0.44			
N	Expt.	0.45	0.45			
	Theor.	0.44	0.44			
O	Expt.	0.48	0.42	0.50		
	Theor.	0.42	0.38	0.42		
F	Expt.	0.40				
	Theor.	0.41				
Ne	Expt.	0.39	0.39	0.45	0.40	0.40
	Theor.	0.40	0.33	0.31	0.33	0.40
Al	Expt.	0.43	0.41			
	Theor.	0.44	0.44			
Cl	Expt.	0.40	0.35	0.33	0.32	
	Theor.	0.41	0.35	0.35	0.41	
Ar	Expt.	0.45	0.33	0.33	0.30	
	Theor.	0.40	0.33	0.31	0.33	

a plasma in full equilibrium. That description is basically different from the one of the independent-electron model. This is easily seen by comparing Eq. (2) of this article with Eqs. (1) and (2) of Ref. 10. Garcia<sup>10</sup> pointed out several difficulties in relating the parameters of the plasma description to those of the beam-foil interaction, and he concluded that although the agreement obtained in some cases is not discouraging, he failed to reproduce the charge-state distribution of nitrogen at 567 keV (see his Fig. 3). As seen from Figs. 4 and 5 of this article, there exists no similar problem in the independent-electron model. Also, Nagel<sup>26</sup> has recently discussed inner-shell excitations in ion-solid interactions and in plasmas and shown that although they are similar in some cases, they are complementary in others. Thus the independent-electron model seems to be superior to the plasma description.

It should be noted that in the independent-electron model the outcome of the beam-solid interaction is expressed in terms of probabilities, and the concept of probabilities is here used as in quantum mechanics and not as in classical statistical mechanics. The use of cross sections

has been avoided. There exists no general expression analogous to Eq. (2) which relates a multitude of cross sections for charge transfer processes to only one parameter, [cf., e.g., Eqs. (72) and (73) of Ref. 25].

In conclusion it can be said that while the results obtained with the independent-electron model are rather satisfactory, this work constitutes only one of the very first steps in a full description of the beam-foil excitation mechanism.

#### ACKNOWLEDGMENTS

The author has received helpful and encouraging comments from Professor T. Andersen, Dr. B. Andresen, Professor H.-D. Betz, Professor G. Brown, Dr. B. Dynefors, Professor J. D. Garcia, Professor T. Huus, Professor J. Lindhard, Professor J. Stoner, Jr. and Dr. B. Winterbon, which in all cases are appreciated, as are computations performed by Dr. B. Helt. Neither the work presented here nor that of Refs. 1-3 would have been possible without the generous hospitality of Professor I. Martinson, which is gratefully appreciated.

<sup>1</sup>B. Dynefors, I. Martinson, and E. Veje, *Phys. Scr.* (to be published).

<sup>2</sup>B. Dynefors, I. Martinson, and E. Veje, *Phys. Scr.* **12**, 58 (1975).

<sup>3</sup>B. Dynefors, I. Martinson, and E. Veje (unpublished).

<sup>4</sup>See, e.g., K. D. Sevier, *Low Energy Electron Spectrometry* (Wiley-Interscience, New York, 1972), pp. 144-153.

<sup>5</sup>I. S. Dmitriev, V. S. Nikolaev, and Ya. A. Teplova, *Phys. Lett.* **27A**, 122 (1968).

<sup>6</sup>I. Martinson, *Phys. Scr.* **9**, 281 (1974).

<sup>7</sup>D. J. Pegg, P. M. Griffin, and I. A. Sellin, in *Atomic Physics*, edited by S. J. Smith and G. K. Walters (Plenum, New York, 1974), Vol. 3, pp. 327-337.

<sup>8</sup>H.-D. Betz, *Rev. Mod. Phys.* **44**, 465 (1972).

<sup>9</sup>W. Brandt, in *Atomic Collisions in Solids*, edited by S. Datz, B. R. Appleton and C. D. Moak (Plenum, New York, 1975), Vol. 1, p. 261.

<sup>10</sup>J. D. Garcia, *Nucl. Instrum. Methods* **110**, 245 (1973).

<sup>11</sup>R. J. Fortner and J. D. Garcia, *Phys. Rev. A* **12**, 858 (1975).

<sup>12</sup>H. G. Berry, L. J. Curtis, D. G. Ellis, and R. M. Schectman, *Phys. Rev. Lett.* **32**, 751 (1974); D. A. Church, in *Invited Papers, Review Papers, and Progress Reports of the Ninth International Conference on the Physics of Electronic and Atomic Collisions*, edited by J. S. Risley and R. Geballe (Univ. of Washington Press, Seattle, 1976), pp. 660-671.

<sup>13</sup>S. Datz, B. R. Appleton, J. A. Biggerstaff, M. D. Brown, H. F. Krause, C. D. Moak, and T. S. Noggle, in Ref. 9, pp. 63-73; and unpublished.

<sup>14</sup>K. E. Pferdekämper and H.-G. Clerc, in Abstracts of Contributed Papers from the Second International Conference on Inner Shell Ionization Phenomena, Freiburg, 1976 (unpublished), p. 112; K. G. Harrison and M. W. Lucas, *Phys. Lett.* **33A**, 142 (1970); **35A**, 402 (1971).

<sup>15</sup>J. R. Oppenheimer, *Phys. Rev.* **31**, 349 (1928).

<sup>16</sup>U. Fano and J. W. Cooper, *Rev. Mod. Phys.* **40**, 441 (1968).

<sup>17</sup>T. A. Carlson and C. W. Nestor, *Phys. Rev. A* **8**, 2887 (1973).

<sup>18</sup>J. H. McGuire and J. R. Macdonald, *Phys. Rev. A* **11**, 146 (1975); D. Storm and D. Rapp, *J. Chem. Phys.* **57**, 4278 (1972); J. F. Reading, *Phys. Rev. A* **8**, 3262 (1973); J. S. Briggs and J. Macek, *J. Phys. B* **5**, 579 (1972); J. H. Macek and J. S. Briggs, *ibid.* **6**, 841 (1973); *Comments At. Mol. Phys.* **4**, 97 (1974).

<sup>19</sup>J. P. Dahl, *The Independent-Particle Model* (Polytechnic, Copenhagen, 1972).

<sup>20</sup>See, e.g., J. C. Slater, *Quantum Theory of Atomic Structure* (McGraw-Hill, New York, 1960), Vol. 1, p. 231.

<sup>21</sup>R. J. Boyd and C. A. Coulson, *J. Phys. B* **6**, 782 (1973).

<sup>22</sup>N. Andersen, G. W. Carriveau, A. F. Glinska, K. Jensen, J. Melskens, and E. Veje, *Z. Phys.* **253**, 53 (1972); B. Dynefors (unpublished).

<sup>23</sup>B. Andresen, K. Jensen, and E. Veje (unpublished).

<sup>24</sup>I. S. Dmitriev, *Zh. Eksp. Teor. Fiz.* **32**, 570 (1957) [*Sov. Phys.-JETP* **5**, 473 (1957)].

- <sup>25</sup>D. H. Madison and E. Merzbacher, in *Atomic Inner-Shell Processes*, edited by B. Crasemann (Academic, New York, 1975), Vol. 1, pp. 51-69.
- <sup>26</sup>D. J. Nagel, in Ref. 9, p. 433.
- <sup>27</sup>P. Hvelplund, E. Laegsgård, J. Ø. Olsen, and E. H. Pedersen, *Nucl. Instrum. Methods* **90**, 315 (1970).
- <sup>28</sup>A. Chateau-Thierry and A. Gladieux, in Ref. 9, p. 307.
- <sup>29</sup>T. M. Buck, L. C. Feldman, and G. H. Wheatley, in Ref. 9, p. 331.
- <sup>30</sup>W. Brandt and R. Sizmann, *Phys. Lett.* **37A**, 115 (1971).  
W. Brandt and R. Sizmann, in Ref. 9, p. 305.
- <sup>31</sup>J. C. Armstrong, J. V. Mullendore, W. R. Harris, and J. B. Marion, *Proc. Phys. Soc. Lond.* **86**, 1283 (1965).  
H. G. Berry, J. Bromander, and R. Buchta, *Nucl. Instrum. Methods* **90**, 269 (1970).
- <sup>32</sup>N. Andersen, W. S. Bickel, R. Boleu, K. Jensen, and E. Veje, *Phys. Scr.* **3**, 255 (1971).
- <sup>33</sup>W. S. Bickel, H. Oona, W. S. Smith, and I. Martinson, *Phys. Scr.* **6**, 71 (1972).
- <sup>34</sup>P. L. Smith and W. Whaling, *Phys. Rev.* **188**, 36 (1969).
- <sup>35</sup>R. Girardeau, E. J. Knystautas, G. Beauchemin, B. Neveu, and R. Drouin, *J. Phys. B* **4**, 1743 (1971).
- <sup>36</sup>M. C. Poulizac, M. Druetta, and P. Ceyzeriat, *J. Quant. Spectrosc. Radiat. Transfer* **11**, 1087 (1971).
- <sup>37</sup>M. Dufay, *Nucl. Instrum. Methods* **90**, 15 (1970).
- <sup>38</sup>H. G. Berry, R. Hallin, R. Sjödin, and M. Gaillard, *Phys. Lett.* **50A**, 191 (1974).
- <sup>39</sup>H. G. Berry, R. M. Schectman, I. Martinson, W. S. Bickel, and S. Bashkin, *J. Opt. Soc. Am.* **60**, 335 (1970).
- <sup>40</sup>W. C. Turkenburg, B. G. Colenbrander, H. H. Kersten, and F. W. Saris, *Surf. Sci.* **47**, 272 (1975).
- <sup>41</sup>N. Bohr, *K. Dan. Vidensk. Selsk. Mat.-Fys. Medd.* **18**, No. 8 (1948). See also Ref. 8.
- <sup>42</sup>K. Taulbjerg, J. S. Briggs, and J. Vaaben, *J. Phys. B* (to be published); K. Taulbjerg, in *Proceedings of the Second International Conference on Inner-Shell Ionization Phenomena*, Freiburg, 1976 (unpublished).
- <sup>43</sup>R. A. Baragiola, P. Ziem and N. Stolterfoht, in Ref. 14, p. 109.